Recruitment of apical dendritic T-type Ca^{2+} channels by backpropagating spikes underlies *de novo* intrinsic bursting in hippocampal epileptogenesis

Yoel Yaari, Cuiyong Yue and Hailing Su

Department of Physiology, Institute of Medical Sciences, Hebrew University-Hadassah School of Medicine, Jerusalem 91120, Israel

A single episode of status epilepticus (SE) induced in rodents by the convulsant pilocarpine, produces, after a latent period of ≥ 2 weeks, a chronic epileptic condition. During the latent period of epileptogenesis, most CA1 pyramidal cells that normally fire in a regular pattern, acquire low-threshold bursting behaviour, generating high-frequency clusters of 3–5 spikes as their minimal response to depolarizing stimuli. Recruitment of a Ni^{2+}- and amiloride-sensitive T-type Ca^{2+} current (I_{CaT}), shown to be up-regulated after SE, plays a critical role in burst generation in most cases. Several lines of evidence suggest that I_{CaT} driving bursting is located in the apical dendrites. Thus, bursting was suppressed by focally applying Ni^{2+} to the apical dendrites, but not to the soma. It was also suppressed by applying either tetrodotoxin or the K$_V$7/M-type K$^+$ channel agonist retigabine to the apical dendrites. Severing the distal apical dendrites $\sim$150 μM from the pyramidal layer also abolished this activity. Intradendritic recordings indicated that evoked bursts are associated with local Ni^{2+}-sensitive slow spikes. Blocking persistent Na$^+$ current did not modify bursting in most cases. We conclude that SE-induced increase in I_{CaT} density in the apical dendrites facilitates their depolarization by the backpropagating somatic spike. The I_{CaT}-driven dendritic depolarization, in turn, spreads towards the soma, initiating another backpropagating spike, and so forth, thereby creating a spike burst. The early appearance and predominance of I_{CaT}-driven low-threshold bursting in CA1 pyramidal cells that experienced SE most probably contribute to the emergence of abnormal network discharges and may also play a role in the circuitry reorganization associated with epileptogenesis.

A variety of brain insults can induce the manifestation of temporal lobe epilepsy, the most common human epileptic syndrome (Engel *et al.* 1997). The processes under-lying temporal lobe epileptogenesis have been studied most extensively in models of status epilepticus (SE) (Morimoto *et al.* 2004). In these animal models, a single episode of SE evoked by chemical or electrical stimulation of mesial temporal lobe structures, causes, after a latent period of several weeks, the emergence of spontaneous seizures. Once these appear, they are sustained for the rest of the animal's life. During the latent period of epileptogenesis, the animals appear behaviourally normal, though electroencephalographic (EEG) recordings disclose the appearance of interictal 'spikes' (Stewart & Leung, 2003). Numerous long-lasting changes in excitatory and inhibitory synaptic functions have been associated with epileptogenesis following SE

(Dudek *et al.* 2002; Morimoto *et al.* 2004). In addition, intrinsic neuronal properties are also persistently altered by SE. Thus, SE induced by the convulsant pilocarpine (pilocarpine-SE) causes a dramatic and enduring increase in the propensity of CA1 (Sanabria *et al.* 2001), subicular (Wellmer *et al.* 2002) and layer V neocortical pyramidal neurons (Sanabria *et al.* 2002) to fire in burst mode. In CA1 cells, where this plasticity phenomenon was first discovered, many regular-firing pyramidal cells convert to a low-threshold bursting mode, generating high-frequency clusters of 3–5 spikes as their minimal response to depolarizing stimuli or even spontaneously (Sanabria *et al.* 2001). The spontaneous bursters, which comprise $\sim$10% of the total neuronal population, serve as the initiators and pacemakers of spontaneous epileptiform bursts, during which the entire CA1 network is engaged in repetitive discharge (Sanabria *et al.* 2001).

Which ionic mechanisms underlie intrinsic bursting in pyramidal neurons that experienced SE (SE-experienced)? A somatic burst is generated when the spike after-depolarization (ADP) is sufficiently large to attain spike threshold and trigger a second spike, which is also followed by a large ADP, and so forth (Jensen *et al.* 1996). In ordinary adult CA1 pyramidal cells, the spike ADP and associated bursting are driven predominantly by persistent Na^+ current (I_{NaP}), as evidenced by their sensitivity to blockers of this current and refractoriness to blockers of Ca^{2+} currents (Azouz *et al.* 1996; Su *et al.* 2001; Yue *et al.* 2005). Yet, intrinsic bursting in most SE-experienced neurons was readily suppressed by low concentrations (50–100 μM) of Ni^{2+}, implicating a Ni^{2+}-sensitive Ca^{2+} current in its generation (Sanabria *et al.* 2001; Su *et al.* 2002). In agreement with this, we have shown a marked and selective up-regulation of the low-voltage-activated (T-type) Ca^{2+} current (I_{CaT}) in SE-experienced neurons (Su *et al.* 2002), assigning I_{CaT} a critical role in bursting. However, the possible contribution of I_{NaP} to this discharge mode was not explored.

Here we combined several experimental approaches to further elucidate the ionic mechanisms underlying the *de novo* intrinsic bursting in SE-experienced CA1 pyramidal cells. Three issues were examined regarding this aberrant activity: (i) the contribution of I_{CaT} *versus* that of the high-voltage-activated R-type Ca^{2+} current (I_{CaR}); (ii) the subcellular localization of the underlying I_{CaT}; and (iii) the contribution of I_{NaP}. Our data show conclusively that bursts arise via activation of I_{CaT} in the apical dendrites by backpropagating somatic spikes. Whereas a secondary contribution of I_{CaR} to bursting cannot be excluded, activation of I_{NaP} does not play a role in this activity in most cases.

Methods

Induction of SE

All animal experiments were conducted in accordance with the guidelines of the Animal Care Committee of the Hebrew University. Male Sabra rats (150–200 g) were injected with the muscarinic agonist pilocarpine (300–380 mg kg^{-1} I.P.), which induced SE in most (~80%) animals (Turski *et al.* 1983; Sanabria *et al.* 2001). Peripheral muscarinic effects were reduced by prior administration of methylscopolamine (1 mg kg^{-1} s.c.; 30 min before injecting pilocarpine). Diazepam (0.1 mg kg^{-1} s.c.) was administered to all animals 2 h after the pilocarpine injection. It terminated the convulsions in the responsive rats and sedated all animals. Within 24 h after pilocarpine injection, the rats appeared behaviourally normal. Both the animals that experienced SE (SE-experienced rats; $n = 49$) and those which did not (control rats; $n = 12$) were used 7–21 days after drug treatment. We have shown

previously that hippocampal slices from SE-experienced rats, but not from control rats, manifest signs of pyramidal cell hyperexcitability (Sanabria *et al.* 2001).

Hippocampal slices

The rats were decapitated under deep isoflurane anaesthesia, and transverse hippocampal slices (400 μm) were prepared with a vibrating microslicer (Leica, Germany) and transferred to a storage chamber perfused with oxygenated (95% O_2–5% CO_2) artificial cerebrospinal fluid (ACSF) containing (mM): NaCl 124, KCl 3.5, $MgCl_2$ 2, $CaCl_2$ 2, $NaHCO_3$ 26 and D-glucose 10, pH 7.4, osmolarity 305 mosmol l^{-1}, where they were maintained at room temperature (20-22°C). Slices were placed one at a time in an interface chamber (33.5°C) and perfused with oxygenated ACSF. In some experiments, as indicated, a deep cut was made in stratum radiatum about 150 μm from, and parallel to, stratum pyramidale (see Fig. 8*A*), using a broken pipette or a razor blade chip propelled by a micromanipulator (Yue *et al.* 2005; Golomb *et al.* 2006). The slices were allowed to recover in the chamber for at least 1 h before initiating a recording session. In most experiments 6-cyano-7-nitro-quinoxaline-2,3-dione (CNQX; 15 μM), 2-amino-5-phosphono-valeric acid (APV; 50 μM) and picrotoxin (100 μM) were added to the ACSF to block fast excitatory and inhibitory synaptic transmission. Other drugs were added to the ACSF as indicated.

Electrophysiological recordings

Intracellular recordings were obtained using sharp glass microelectrodes containing 4 M potassium acetate (90–110 MΩ) and an amplifier (Axoclamp 2B, Axon Instruments, Union City, CA, USA) that allowed simultaneous injection of current and measurement of membrane potential. The bridge balance was carefully monitored and adjusted before each measurement. The intracellular signals were filtered on-line at 10 kHz, digitized at a sampling rate of 10 kHz or more, and stored on a personal computer using a data acquisition system (Digidata 1322A) and pCLAMP software (Axon Instruments).

Drug applications

Drugs were applied to the whole slice by bath application or to selected locations in the slice using a puff application system. Because the spread of drugs in slices maintained in an interface chamber is predominantly by diffusion, the onset and offset of drug effects are slow (of the order of tens of minutes). For all bath-applied drugs used in this study, maximal effects were obtained within 20–30 min of adding them to the ACSF.

For focal drug applications we used, as in previous studies (Chen *et al.* 2005; Yue *et al.* 2005; Yue & Yaari, 2006), a puffing system consisting of a pneumatic pump (Pico-spritzer III, General Valve, Fairfield, NJ, USA) connected to a patch pipette (tip diameter, $\sim$10 μm). The pipette was filled with ACSF containing the drug to be applied at 10-fold higher concentration than that required in bath-application experiments. The tip of the pipette touched the upper surface of the slice. Drugs were applied using pressure pulses of 5 bars lasting 20 ms. These pulses produced a drop that covered a circular area $\sim$50 μm in diameter when ejected onto the surface of the slice (visualized by including fast-green dye in the pipette solution). To apply drugs to the region of the soma and axon initial segment (a region we refer to here as axo-soma though it may include to some extent also proximal apical and basilar dendrites), the puffing pipette was positioned in stratum pyramidale about 25 μm from the recording microelectrode (lodged in the soma of the neuron). To apply drugs to the distal apical dendrites, the puffing pipette was positioned in stratum radiatum about 200–300 μm away from, and vertical to, the stratum pyramidale. Likewise, to apply drugs to the basal dendrites, the puffing pipette was positioned in stratum oriens about 100 μm away from, and vertical to, the stratum pyramidale. This experimental arrangement is shown below in Fig. 4*A*. The effects of focally applied drugs, when present, appeared usually within 3 min of puffing, and reached a maximum within 8–10 min. These delays are undoubtedly due to slow diffusional spread of the drugs from their superficial site of application into the slice.

Chemicals and drugs

Stock solutions of 4β-phorbol 12,13-dibutyrate (PDB; 10 mM) and riluzole (10 mM) were prepared in dimethyl sulfoxide (DMSO) and stored at $-20°$C. They were usually diluted at 1 : 1000 when added to the ACSF. The ACSF contained equal amounts of DMSO (0.001%), which by itself had no effects on the measured parameters. All other drugs were added to the ACSF from aqueous stock solutions. Chemicals and drugs were obtained from Sigma (Petach-Tikva, Israel), except for SNX-482 (Alomone Laboratories, Jerusalem, Israel).

Cell staining

Cell somata or putative apical dendrites of CA1 pyramidal cells were injected with biocytin. Following the experiment, the slices were fixed overnight in 4% paraformaldehyde, cut into thin (120 μm) slices and incubated with avidin-biotin complex (Vectastain ABC Elite kit, Vector).

Analysis

To measure passive membrane properties, the pyramidal cells were injected with small (0.1–0.5 nA) 200 ms negative current pulses. The apparent input resistance was provided by the slope of the linear regression line fitted through the linear portion of the steady-state voltage–current amplitude plot. Spike threshold was defined as the membrane potential where the slope of the voltage trace increased abruptly during membrane charging induced by prolonged positive current pulses. The fast spike after-hyperpolarization (fAHP) was measured as the potential attained at the end of the spike downstroke. The size of the subthreshold depolarizing potential (SDP) was measured as the integrated 'area under the curve' between the end of the stimulus artifact and the point at which membrane voltage returned to resting potential.

Averaged data are expressed as mean $\pm$ S.E.M. The significance of the differences between the measured parameters was evaluated using paired Student's *t* test with a significance level of 0.05.

Terminology

In this study of bursting we focus only on neurons that generate a burst as their minimal response to depolarizing current pulses. We have previously referred to these neurons as 'low-threshold' bursters, to differentiate them from neurons that generate burst-like responses when stimulated with 2–3 times threshold depolarizing current pulses (referred to as 'high-threshold' bursters; Jensen *et al.* 1994, 1996; Su *et al.* 2001). High-threshold bursting is found in both normal and SE-experienced CA1 pyramidal cells and its mechanism has been thoroughly investigated (Yue *et al.* 2005).

Results

De novo bursting in SE-experienced CA1 pyramidal cells

The SE-experienced and control rats were killed for *in vitro* experiments 7–21 days after drug treatment. The data here were collected from 32 SE-experienced rats (98 neurons in 80 slices) and seven control rats (22 neurons in 15 slices). The neurons were impaled with sharp glass microelectrodes for current-clamp recordings of passive and active neuronal membrane properties. The mean values in the SE-experienced and control neurons, respectively ($n = 20$ in both groups), of resting membrane potential (66.3 $\pm$ 0.8 and 65.8 $\pm$ 0.9 mV) and apparent input resistance (34.2 $\pm$ 1.2 and 36.2 $\pm$ 1.2 MΩ), as well as of spike threshold (-53.3 ± 1.1 and -53.1 ± 1.2 mV), amplitude (90.2 $\pm$ 2.0 and 90.4 $\pm$ 1.4 mV) and width (1.9 $\pm$ 0.2 and 2.0 $\pm$ 0.1 ms), were similar. In all neurons,

spikes evoked by brief (4 ms) threshold-straddling depolarizing current pulses repolarized to a membrane potential about 10 mV more positive than resting potential (-53.3 ± 1.2 and -54.7 ± 1.4 mV in SE-experienced and control neurons, respectively; $n = 20$); the so-called fast afterhyperpolarization (fAHP). Following the fAHP the membrane potential declined monotonically to baseline or, in most cases, first repolarized again and then declined slowly to baseline, creating an 'active' spike ADP.

In 42 of 65 sampled SE-experienced neurons (65%), the spike ADP was sufficiently large to trigger additional spikes, thus producing a spike burst. The fraction of bursting neurons was about the same in slices obtained during the second week (7–14 days: 23 of 35; 66%) and third week (15–21 days: 19 of 30; 64%) after pilocarpine-SE. The number of intraburst spikes varied between 3 and 5, averaging 3.6 ± 0.1 spikes. The intraburst firing frequency ranged between 144.1 and 377.2 Hz, averaging 231.2 ± 9.9 Hz ($n = 30$). In many of these neurons, such as the one illustrated in Fig. 1, the timing of individual intraburst spikes displayed a jitter, which was more pronounced in the late part of long (> 3 intraburst spikes) bursts (Fig. 1*A–C* and overlaid traces in Fig. 1*D*). In some neurons, failure of one of the late spikes revealed an underlying small subthreshold 'hump' (see arrows in Fig. 1*B* and *C*). In contrast to the SE-experienced neurons, none of the control neurons generated a spike burst when similarly depolarized.

Adding 100 μM Ni^{2+} to the ACSF progressively converted bursting to single spiking in eight of 10 bursting SE-experienced neurons (Fig. 1*E–G*). In the remaining two neurons, bursting persevered though the number of intraburst spikes was reduced from 3 to 2 spikes in one neuron. Raising the Ni^{2+} concentration to 1 mM also did not suppress bursting in these two neurons (data not shown). Altogether, Ni^{2+} reduced the number of intraburst spikes from 3.9 ± 0.3 to 1.4 ± 0.3 ($n = 10$; $P < 0.005$). These findings confirm that bursting emerging early in epileptogenesis is driven by a Ni^{2+}-sensitive Ca^{2+} current.

Effects of amiloride and SNX-482

Low concentrations (50–100 μM) of Ni^{2+} block I_{CaT}, as well as I_{CaR} (Williams *et al.* 1999; Lee *et al.* 1999). We have previously shown that the density of I_{CaT} is strongly up-regulated early after pilocarpine-SE, whereas that of I_{CaR} is unchanged. Moreover, the up-regulated I_{CaT} is highly sensitive to Ni^{2+} (IC$_{50}$ ~25 μM; Su *et al.* 2002). Of the three α_1 subunits generating I_{CaT} (Ca$_V$3.1, Ca$_V$3.2 and Ca$_V$3.3), Ca$_V$3.2 is 20-fold more sensitive to Ni^{2+} (IC$_{50}$, 13 μM) than the other two isoforms (Lee *et al.* 1999). Together, these findings suggested that Ca$_V$3.2 T-type Ca^{2+}
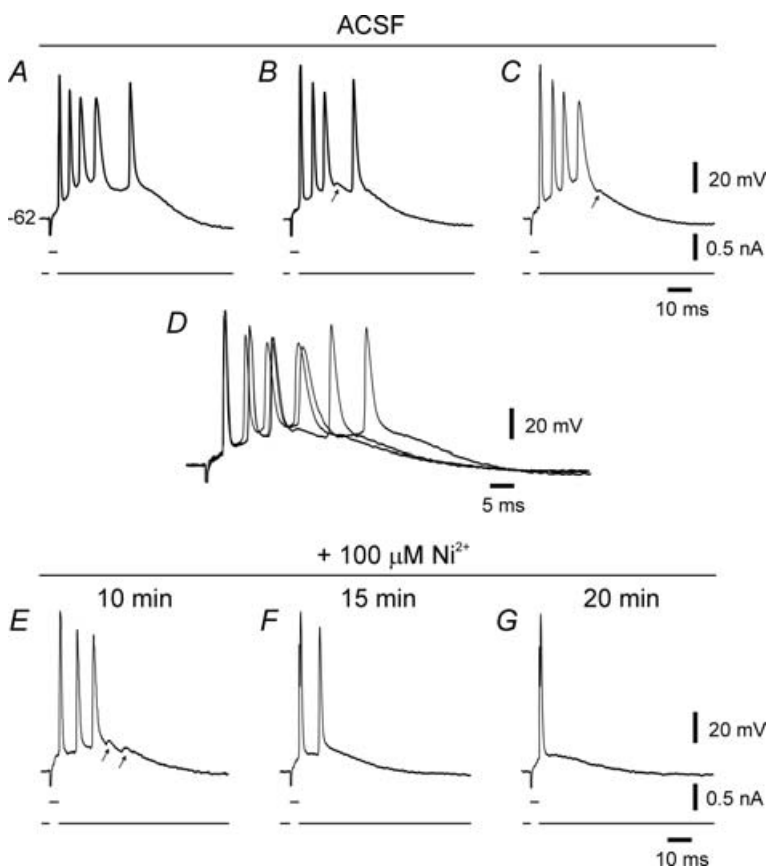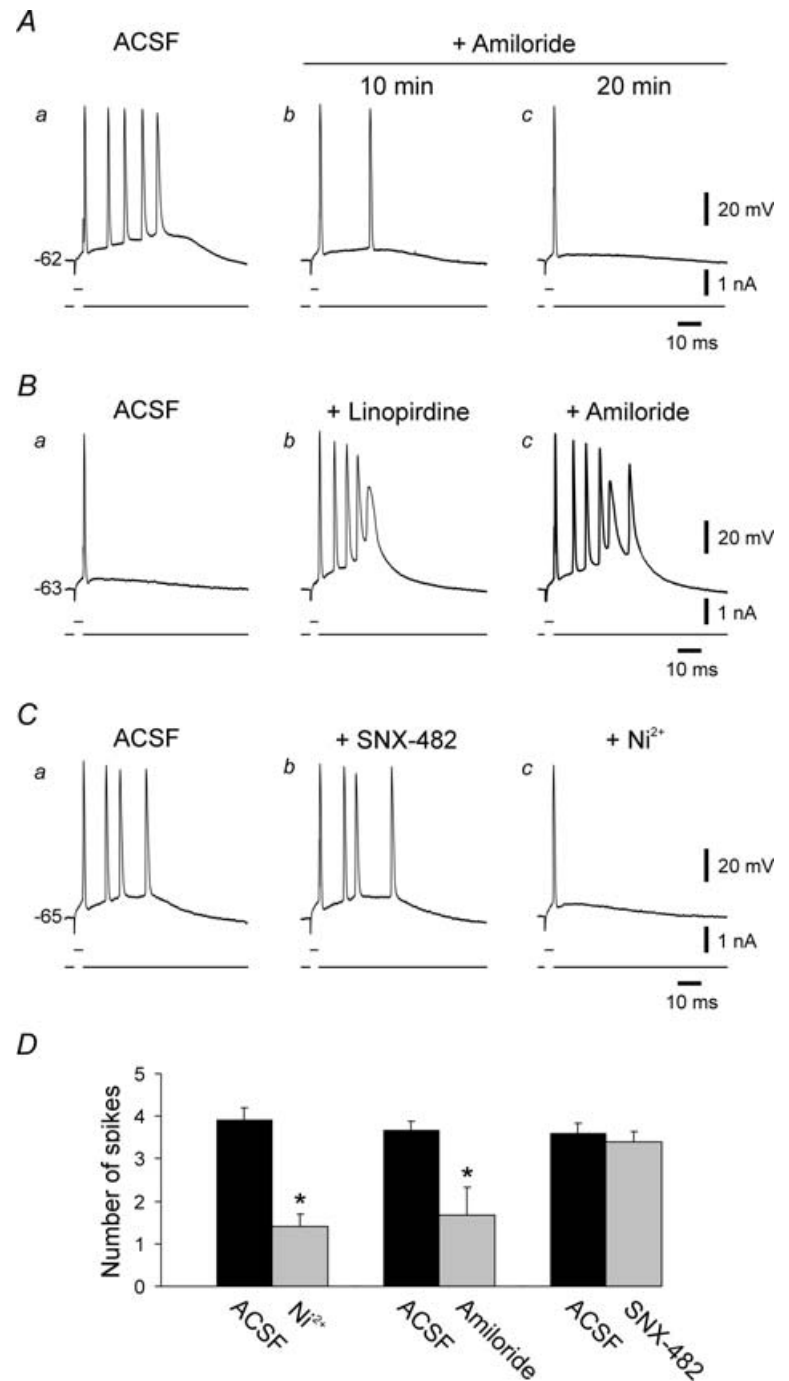

Figure 1. Low-threshold bursting in an SE-experienced CA1 pyramidal cell
The experiment was performed 7 days after pilocarpine-SE. In this and in subsequent figures, the bottom trace in each panel depicts the stimulus waveform, whereas the top trace shows the voltage response. The resting potential of the neuron is indicated to the left of the uppermost voltage trace. Brief stimuli evoked bursts of 4–5 spikes (*A–C*; these traces are expanded and overlaid in *D* to facilitate comparison). Note jitter in spike timing, particularly of later spikes. Spike failure during a burst sometimes revealed a small subthreshold 'hump' (see arrows in *B, C* and *E*). Adding 100 μM Ni^{2+} to the ACSF caused progressive suppression of bursting (*E–G*).

channels provide the critical depolarization for bursting in SE-experienced neurons. To further assess the roles of I_{CaT} and I_{CaR} in this discharge behaviour, we monitored the effects of amiloride, known to block I_{CaT} preferentially over high-voltage activated Ca^{2+} currents (Tang *et al.* 1988; Takahashi *et al.* 1989; Scroggs & Fox, 1992; Williams *et al.* 1997; Todorovic & Lingle, 1998; Kim & Chung, 1999; Ikeda & Matsumoto, 2003), and to block $Ca_V3.2$ (IC_{50}, 167 μM; Williams *et al.* 1999) preferentially over $Ca_V3.1$ (IC_{50} value in the millimolar range; Lacinová *et al.* 2000).

It is important to note that amiloride (up to 500 μM) was ineffective in blocking I_{CaR}, while strongly blocking I_{CaT} in the same neurons (Hilaire *et al.* 1997). In 4 out of 5 SE-experienced neurons, as illustrated in Fig. 2*A*, adding 300 μM amiloride to the ACSF converted bursting to single spiking within 20 min. In the fifth neuron, the number of intraburst spikes actually increased from 4 to 5 spikes. Altogether, amiloride reduced the average number of intraburst spikes from 3.6 ± 0.2 to 1.8 ± 0.8 ($n = 5$; $P < 0.05$).

Figure 2. Effects of amiloride and SNX-482 on bursting
A, exposure of a bursting SE-experienced neuron (five intraburst spikes; *Aa*) to 300 μM amiloride gradually suppressed bursting; after 20 min exposure the neuron generated a solitary spike (*Ab* and *c*). *B*, exposure of regular firing control neuron (*Ba*) to ACSF containing 10 μM linopirdine induced bursting (five intraburst spikes) within 20 min (*Bb*). Addition of 300 μM amiloride to the ACSF enhanced bursting (six intraburst spikes; *Bc*). Bursting persisted throughout the 45 min exposure to this drug combination. *C*, exposure of another bursting SE-experienced neuron (four intraburst spikes; *Ca*) to 1 μM SNX-482 for 45 min did not modify it bursting mode (*Cb*). Subsequent addition of 100 μM Ni^{2+} to the ACSF converted bursting to single spiking within 20 min (*Cc*). *D*, bar histogram summarizes the effects of 100 μM Ni^{2+}, 300 μM amiloride and 1 μM SNX-482 on bursting SE-experienced neurons. Both Ni^{2+} and amiloride caused significant suppression of bursting (indicated with asterisks).

The disadvantage of using amiloride to characterize the function of I_{CaT} is that it also blocks Na^+–H^+ and Na^+–Ca^{2+} exchangers (Kleyman & Cragoe, 1988) and acid-activated ion channels (Waldman *et al.* 1997). To evaluate the possibility that these actions may be responsible for amiloride-induced burst suppression in SE-experienced neurons, we examined its effects in four control neurons on bursting induced by linopirdine (Yue & Yaari, 2004), a selective blocker of K_V7 (KCNQ) channels that generate neuronal M-type K^+ current (I_M; Robbins, 2001). As shown in Fig. 2*B*, linopirdine-induced bursting (Fig. 2*Ba* and *b*) was not suppressed by amiloride (up to 45 min exposure) and was even enhanced in this particular neuron (Fig. 2*Bc*), as well as in another one. Altogether, amiloride increased the average number of intraburst spikes from 4.0 ± 0.4 to 4.5 ± 0.6, but this effect was not statistically significant.

We also examined the effects of SNX-482 on bursting in SE-experienced neurons. This spider toxin variably reduces I_{CaR} in different types of brain neurons by blocking several isoforms of $Ca_V2.3$ subunits (Wilson *et al.* 2000; Tottene *et al.* 2000; Sochivko *et al.* 2002). Perfusion with ACSF containing $1\,\mu M$ SNX-482 (which blocks $\sim 50\%$ of I_{CaR} in rat CA1 pyramidal cells; Sochivko *et al.* 2003) for up to 45 min did not affect bursting in 4 out of 5 neurons (Fig. 2*Ca* and *Cb*). In the fifth neuron, the number of intraburst spikes decreased from 5 to 4 spikes. In three of the neurons, $100\,\mu M$ Ni^{2+} was added following exposure to SNX-482, resulting in burst suppression (Fig. 2*Cc*). Overall, there were no statistically significant effects of SNX-482 on the number of intraburst spikes (3.6 ± 0.2 before *versus* 3.4 ± 0.2 after exposure to SNX-482).

The most parsimonious conclusion from these data, summarized in Fig. 2*D*, is that I_{CaT}, particularly $Ca_V3.2$, provides a critical depolarizing drive for bursting in SE-experienced CA1 pyramidal cells. However, because SNX-482 only partially blocks I_{CaR} in these neurons (Sochivko *et al.* 2003), we cannot exclude an auxiliary contribution of I_{CaR} to this aberrant activity.

Effects of PDB and riluzole

Another current that may contribute to bursting is I_{NaP} (French *et al.* 1990; Yue *et al.* 2005). In normal CA1 pyramidal cells, I_{NaP} drives bursting induced by high-K^+ or low-Ca^{2+} ACSFs (Azouz *et al.* 1996; Su *et al.* 2001) or by blocking M-type K^+ channels (Yue & Yaari, 2006). This current also contributes critically to bursting in developing CA1 pyramidal cells in synergy with various Ca^{2+} currents (Chen *et al.* 2005; Metz *et al.* 2005).

We assessed the contribution of I_{NaP} by monitoring the effects of the protein kinase C activator PDB and the neuro-protective drug riluzole. In CA1 pyramidal cells these drugs block I_{NaP} completely in doses that only mildly reduce transient Na^+ current (Yue *et al.* 2005). To validate the block of I_{NaP} by PDB and riluzole in these experiments, we monitored not only spiking activity, but also the sub-threshold depolarizing potentials (SDPs) evoked by brief threshold-straddling stimuli that fail to trigger spikes (Azouz *et al.* 1996; Su *et al.* 2001). These potentials, lasting 50–100 ms, are probably driven by I_{NaP} because they are readily suppressed by tetrodotoxin (TTX), as well as by more-selective I_{NaP} blockers, but are resistant to blockade of voltage-gated Ca^{2+} currents (Azouz *et al.* 1996; Su *et al.* 2001).

As illustrated in Fig. 3*A*, bursting in an SE-experienced neuron was unaffected by $5\,\mu M$ PDB applied in the ACSF for up to 1 h (Fig. 3*Aa*1 and *b*1). Yet, within 12 min of exposure to PDB, the SDP was reduced to a passive membrane response (Fig. 3*Aa*2 and *b*2 and overlaid traces in Fig. 3*Ad*). Subsequent addition of $100\,\mu M$ Ni^{2+} to the PDB-containing ACSF converted bursting (three intra-burst spikes) to single spiking within 15 min (Fig. 3*Ac*1). Similar results were obtained in 4 out of 5 neurons exposed sequentially to $5\,\mu M$ PDB and Ni^{2+}. In the exceptional neuron, exposure to $5\,\mu M$ PDB converted the neuron from bursting (three intraburst spikes) to single spiking (data not shown). Altogether, PDB suppressed the SDPs by $45.4 \pm 6.1\%$ (from 216.6 ± 25.7 to 94.1 ± 8.1 mV ms; $P < 0.005$). Adding $10\,\mu M$ riluzole to the ACSF also did not affect bursting in 4 out of 4 SE-experienced neurons (Fig. 3*Ba*1 and *b*1), while suppressing the SDPs in all of them by $53.7 \pm 5.7\%$ (from 191.1 ± 10.2 to 104.3 ± 5.7 mV ms; $P < 0.005$; Fig. 3*Ba*2 and *b*2). Again, subsequent addition of $100\,\mu M$ Ni^{2+} converted bursting to single spiking in all cases (Fig. 3*Bc*1).

Together, these data indicate that I_{NaP} activation is not mandatory for bursting in most cases. Nonetheless, in the small fraction of bursting neurons ($\sim 20\%$) that are not suppressed by Ni^{2+}, I_{NaP} may play a dominant role in burst production.

Focal applications of Ni^{2+}

In ordinary adult CA1 pyramidal cells, I_{CaT} is located predominantly in the distal apical dendrites, as it disappears entirely by truncating them at a distance of $150\,\mu m$ from the soma (Karst *et al.* 1993). We speculated that the up-regulated I_{CaT} driving bursting in SE-experienced neurons is also located in the distal apical dendrites. To test this notion, we first monitored the effects of Ni^{2+} focally applied to various parts of bursting neurons. The experimental arrangement is illustrated in Fig. 4*A* (see Methods; Chen *et al.* 2005; Yue *et al.* 2005; Yue & Yaari, 2006). The application pipette was filled with ACSF containing $5\,m M$ Ni^{2+}. Two representative experiments are shown in Fig. 4 *B* and *C*. In the first experiment,

recordings were made from a neuron generating bursts of 3 spikes in response to brief depolarizing current pulses. Applying Ni^{2+} to the axo-soma had no effect on bursting (Fig. 4Ba1 and b1). By contrast, 3 min after puffing Ni^{2+} onto the apical dendrites at a distance $\sim300\ \mu$m from the soma, bursting was suppressed (Fig. 4Bc1). Similar results were obtained in 5 out of 6 experiments. In the sixth experiment, focal applications of Ni^{2+}, followed by bath application of 100 μM Ni^{2+}, exerted no effects on bursting (data not shown). The SDPs were unaffected by the focal applications of Ni^{2+} (Fig. 4Ba2–c2 and overlaid traces in Fig. 4Bd).

In another series of three experiments we applied Ni^{2+} sequentially to three regions: apical dendrites, axo-soma and basal dendrites. As shown in Fig. 4C, bursting (five intraburst spikes; Fig. 4Ca) was converted to single spiking 3 min after puffing Ni^{2+} onto the apical dendrites (Fig. 4Cb). This blocking effect subsided after another 10 min and the neuron recovered its bursting behaviour (Fig. 4Cc). The application pipette was then moved proximally. Applying Ni^{2+} to the axo-soma had no effect on bursting (Fig. 4Cd). After another 10 min the application pipette was moved to stratum oriens at $\sim100\ \mu$m from the recording microelectrode and Ni^{2+} was reapplied. Again, no change was seen (Fig. 4Ce).

Simply puffing ACSF on the apical dendrites of SE-experienced neurons had no effect on bursting during the subsequent 15 min observation period ($n = 4$; data not shown). Together, these observations strongly suggest that burst generation requires activation of I_{CaT} in the distal apical dendrites.
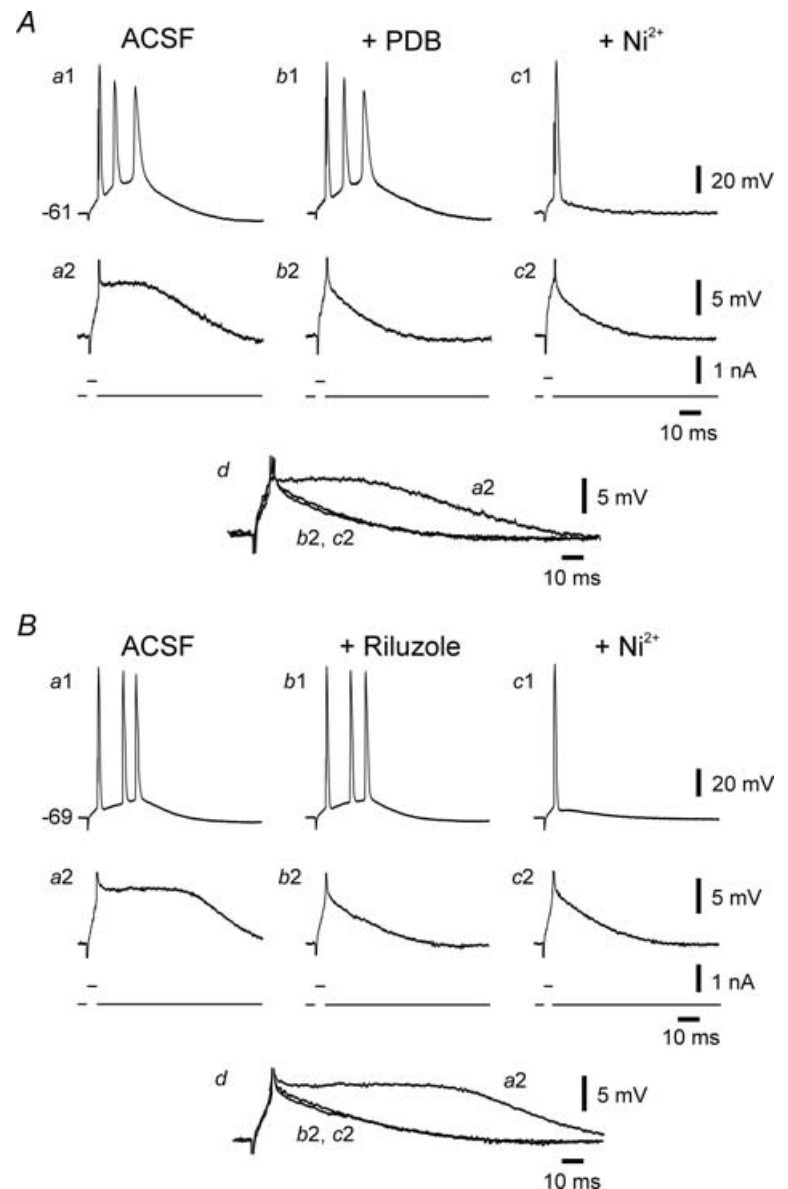

Figure 3. Bursting in SE-experienced neurons is resistant to 4β-phorbol 12,13-dibutyrate (PDB) and riluzole

A, exposure of the first burster (three intraburst spikes; Aa1) to 5 μM PDB for 30 min exerted no effect on the bursting (Ab1), even though the large SDP (Aa2) was suppressed (Ab2). Addition of 100 μM Ni^{2+} to the ACSF within 25 min converted bursting to single spiking (Ac1), while the SDP was not further affected (Ac2). The traces of the SDPs (Aa2, b2 and c2) are expanded and overlaid in Ad to facilitate comparison. B, exposure of another bursting neuron (Ba1) to 10 μM riluzole for 30 min exerted no effect on the bursting behaviour (three intraburst spikes) of the neuron (Bb1) even though the large SDP (Ba2) was suppressed (Bb2). Addition of 100 μM Ni^{2+} to the ACSF within 25 min converted bursting to single spiking (Bc1), while the SDP was not further affected (Bc2). The traces of the SDPs (Ba2, b2 and c2) are expanded and overlaid in Bd to facilitate comparison.

Focal applications of TTX

Recruitment of Ca^{2+} channels in apical dendrites by a spike initiated at the proximal axon is facilitated by its active backpropagation (Spruston *et al.* 1995). Hence, blocking spike backpropagation should interfere with bursting that depends on apical dendritic Ca^{2+} currents (Magee & Carruth, 1999; Chen *et al.* 2005; Yue & Yaari, 2006). We tested this prediction in five SE-experienced bursting neurons by puffing TTX on their apical dendrites. The application pipette was filled with 50 nM TTX. A representative experiment is shown in Fig. 5. Within 5 min of TTX application, bursting (four intraburst spikes) was converted to single spiking (Fig. 5*Aa* and *Ab*). At the same

time, the SDPs evoked by identical stimuli, were only minimally affected (Fig. 5*Ba* and *Bb*, and overlaid races in Fig. 5*Bd*). Likewise, the rise time and amplitude of the primary spike were unchanged (inset in Fig. *Ad*). The latter observations confirm that TTX blocked bursting by acting at distal portions of the neuron. The application pipette was then moved to the axo-soma and TTX was re-applied. After 4 min, the spike ADP (Fig. 5*Ac*, and overlaid traces in Fig. 5*Ad*) and the SDPs were strongly suppressed (Fig. 5*Bc*, and overlaid races in Fig. 5*Bd*). These latter effects concurred before any noticeable change in the rise time or amplitude of the primary spike (inset in Fig. 5*Ad*), suggesting that they are due to block of I_{NaP} (Yue *et al.*
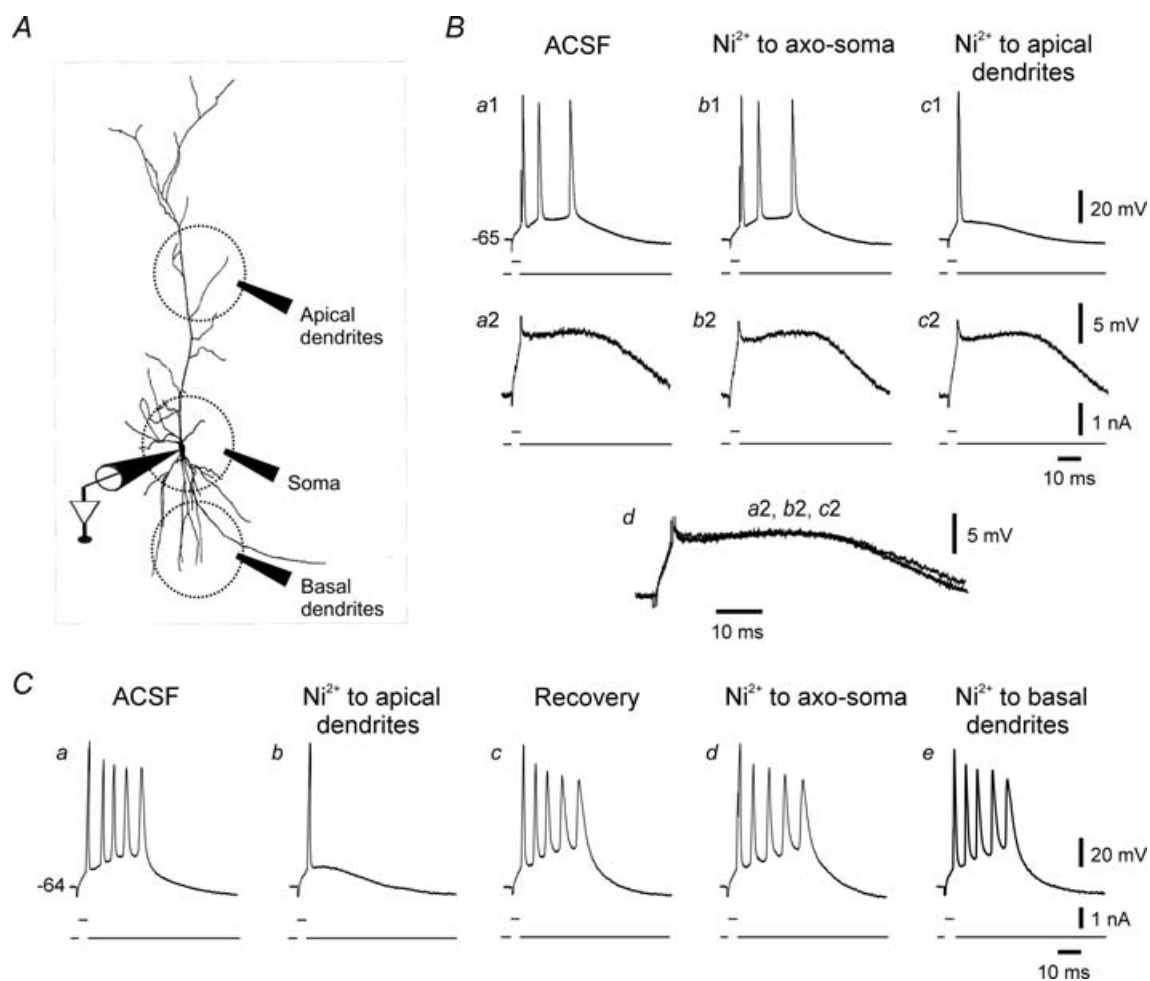

Figure 4. Effects of focal applications of Ni^{2+} on bursting

A, scheme of experimental arrangement for focal pressure application of drugs (see Methods). *B*, this neuron generated a burst of 3 spikes in response to brief stimuli (*Ba*1). Brief, threshold-straddling pulses that failed to elicit a spike evoked a prolonged SDP (*Ba*2). Focal application of Ni^{2+} to the axo-soma had no effect on any of the spiking or subthreshold responses (*Bb*1 and *b*2). In contrast, when Ni^{2+} was applied to the apical dendrites, bursting was suppressed after 3 min (*Bc*1). Yet at the same time, the SDP was unchanged (*Bc*2; see also *Bd* in which portions from traces *Ba*2, *Bb*2 and *Bc*2 are expanded and overlaid). *C*, in another neuron firing in bursts of 5 spikes (*Ca*), Ni^{2+} was focally applied in the reversed order. When puffed on the apical dendrites, Ni^{2+} promptly suppressed bursting (*Cb*). This effect recovered after 10 min (*Cc*). Then Ni^{2+} was applied to the axo-soma (*Cd*) and after another 10 min to the basal dendrites (*Ce*). Neither of the latter applications suppressed bursting.

2005), which is 4-fold more sensitive to TTX than the transient Na^+ current generating the fast spike (Hammarstrom & Gage, 1998). Several minutes later, however, the primary spike also decreased and eventually was blocked entirely. Similar results were obtained in 4 out of 5 experiments. In the fifth experiment, dendritic applications of TTX failed to affect bursting; subsequent axo-somatic application suppressed bursting before diminishing the primary spike (data not shown). On average, the SDPs were unaffected by dendritic applications of TTX (224.0 ± 22.0 *versus* 221.8 ± 20.4 mV ms), but were reduced to $40.9 \pm 3.5\%$ after its axo-somatic application (88.8 ± 6.6 mV ms; $n = 5$; $P < 0.005$).

These data suggest that somatic spike backpropagation into the apical dendrites is a critical step in burst electrogenesis in SE-experienced neurons. It is unlikely that TTX suppressed bursting by blocking critical I_{NaP} in the apical dendrites, because, as shown above (Fig. 3), the I_{NaP} blockers PDB and riluzole applied to the entire neuron in the superfusing ACSF did not affect this firing mode.

Focal applications of retigabine

To further assess the role of dendritic Ca^{2+}-dependent electrogenesis in bursting, we tested the effects of retigabine applied to the distal apical dendrites. Retigabine is an agonist of K_V7/M-type K^+ channels, enhancing I_M by strongly shifting its activation curve to more negative potentials (Main *et al.* 2000; Wickenden *et al.* 2000; Tatulian *et al.* 2001). We have shown previously that retigabine applied to the apical dendrites of normal CA1 pyramidal cells locally suppresses dendritic Ca^{2+} spikes and Ca^{2+}-dependent bursting induced by 4-aminopyridine without affecting spike generation in the axo-soma (Yue & Yaari, 2006).

The application pipette was filled with $100 \, \mu M$ retigabine. A representative experiment is shown in Fig. 6. After 6 min of applying retigabine to the apical dendrites, bursting (four intraburst spikes) was converted to single spiking (Fig. 6*Aa* and *Ab*). Despite the suppression of bursting, the SDPs were unaffected (Fig. 6*Ba* and *Bb*, and overlaid races in Fig. 6*Bd*). Likewise, resting potential and apparent input resistance were unaffected by distally applied retigabine (Yue & Yaari, 2006). The application pipette was then moved to the axo-soma and retigabine was re-applied. This application hyperpolarized the neuron from -71.0 to -75.4 mV within 5 min. We counteracted this hyperpolarization by steadily injecting appropriate positive current. Under this condition the spike ADP was further reduced (Fig. 6*Ac*, and overlaid traces in Fig. 6*Bd*) and the SDPs were markedly suppressed (Fig. 6*Bc*, and overlaid traces in Fig. 6*Bd*). Similar results were obtained in 4 out of 4 experiments. On average, the SDPs were unaffected by dendritic applications
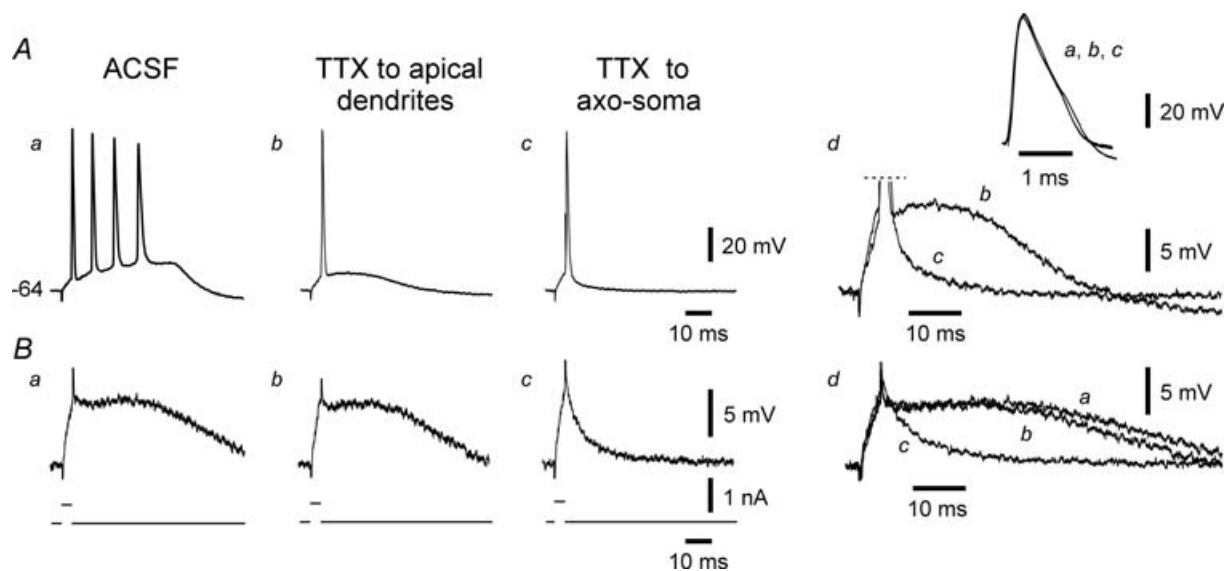

Figure 5. Effects of focal applications of TTX on bursting
This neuron generated a burst of 4 spikes in response to brief stimuli (*Aa*). Brief, threshold-straddling pulses that failed to elicit a spike evoked a prolonged SDP (*Ba*). Focal application of TTX to the distal apical dendrites within 5 min suppressed bursting (*Ab*), but not the SDP (*Bb*). When applied to the axo-soma, TTX within 4 min further reduced the spike ADP (*Ac*; see also *Ad* in which portions from traces *Ab* and *Ac* are expanded and overlaid for comparison) and suppressed the SDP (*Bc*; see also *Bd* in which portions from traces *Ba*, *Bb* and *Bc* are expanded and overlaid). These latter effects concurred without a significant change in the rise time or amplitude of the primary spike (*Ad*, inset, showing expanded and overlaid traces from *Aa*, *Ab* and *Ac*). After 5 min, all spiking was blocked (not shown).

of retigabine (234.3 ± 30.0 *versus* 218.4 ± 25.1 mV ms), but were reduced to $43.3 \pm 5.0\%$ after its axo-somatic application (92.2 ± 8.2 mV ms; $n = 4$; $P < 0.05$).

These data confirm that bursting in SE-experienced neurons requires interplay between axo-somatic and apical dendritic conductances, and can be suppressed by increasing I_M conductance in the apical dendrites.

Intradendritic recordings

To further assess the role of apical dendrites in bursting, we performed intradendritic recordings from putative apical dendrites of SE-experienced and of control CA1 pyramidal cells. Cells were impaled in stratum radiatum about 200 μm from the cell body layer, and biocytin was injected via the recording microelectrode for *post hoc* histological verification of cell type. Successful staining was obtained in 6 out of 8 and 3 out of 4 impalements from SE-experienced and control neurons, respectively. In all cases the stained neuron had its soma in the pyramidal layer and manifested characteristic pyramidal cell morphology (Fig. 7A). In 3 out of 6 confirmed intradendritic recordings from SE-experienced neurons, the primary fast spike was followed by a series of fast and slow spikes. A representative example of such complex spiking is shown in Fig. 7B. It can be seen in the three sequential responses (Fig. 7Ba1–a3, overlaid in Fig. 7Ba4) that the late slow spikes (presumed to be Ca^{2+} spikes) show considerable jitter from one response to another. Addition of 100 μm Ni^{2+} to the ACSF progressively reduced the burst responses until they were reduced to a single spike (Fig. 7Bb1–b4). In the other three

recordings from the SE-experienced neurons (Fig. 7C), as well as in the three confirmed intradendritic recordings from control neurons, brief depolarizing current pulses evoked a solitary spike that was followed by a monotonically declining ADP.

Our findings are consistent with previous studies showing that backpropagating spikes do not normally evoke bursts or Ca^{2+} spikes in the apical dendrites (Spruston *et al.* 1995; Magee & Carruth, 1999). However, we show here that early after pilocarpine-SE, these dendrites manifest a heightened propensity for generating Ca^{2+}-dependent bursts and Ca^{2+} spikes upon their invasion by backpropagating fast spikes.

Truncation of distal apical dendrites

As a final test of the active role played by the apical dendrites in the bursting behaviour of SE-experienced neurons, we examined the consequences of truncating these dendrites. Somatic intracellular recordings were made > 1 h after surgically cutting the apical dendrites at about 150 μm from the soma (Fig. 8A; see Methods). We have shown previously that truncated CA1 pyramidal cells remain viable and normally excitable (Yue *et al.* 2005). Of 22 truncated SE-experienced neurons, only one (5%) neuron fired bursts as its minimal spike output (compared to 65% in intact SE-experienced neurons), whereas all other neurons generated a solitary spike (Fig. 8B). Notwithstanding, the latter neurons readily converted to bursting mode after linopirdine (10 μM) was added to the ACSF ($n = 4$; data not shown), as shown for normal intact neurons (Yue &
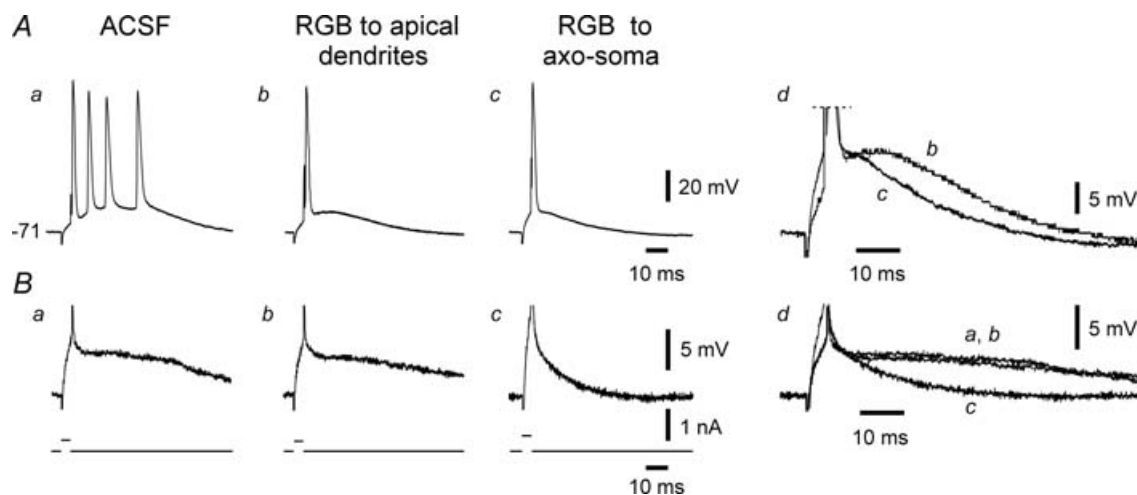

Figure 6. Effects of focal applications of retigabine on bursting
This neuron generated a burst of 4 spikes in response to brief stimuli (*Aa*). Brief, threshold-straddling pulses that failed to elicit a spike evoked a prolonged SDP (*Ba*). Focal application of retigabine (RGB) to the distal apical dendrites within 6 min suppressed bursting (*Ab*), but not the SDP (*Bb*). When applied to the axo-soma, retigabine further reduced the spike ADP (*Ac*; see also *Ad* in which portions from traces *Ab* and *Ac* are expanded and overlaid for comparison) and suppressed the SDP (*Bc*; see also *Dd* in which portions from traces *Ba*, *Bb* and *Bc* are expanded and overlaid).

Yaari, 2004), as well as for control intact neurons in this study (see above, Fig. 2*Ba* and *b*). These results further support our hypothesis the bursts in SE-experienced neurons result from interplay between somatic and apical dendritic conductances.

Discussion

In this study we further explore the mechanism of low-threshold bursting that emerges in CA1 pyramidal cells after pilocarpine-SE (Sanabria *et al.* 2001). We show that this aberrant firing mode, which greatly amplifies the spike output of SE-experienced neurons, predominates already during the second week after pilocarpine-SE before the emergence of spontaneous seizures (> 2 weeks after pilocarpine-SE; Turski *et al.* 1983; Priel *et al.* 1996). We confirm the predominant and critical role of I_{CaT} in bursting and show that bursts are the product of interplay between backpropagating Na^+ spikes and I_{CaT}-driven depolarizations in the distal apical dendrites. A comparable 'ping-pong' mechanism underlies low-threshold bursting that appears in CA1 pyramidal cells during the second and third postnatal weeks (Chen *et al.* 2005). Thus, our findings highlight a similarity
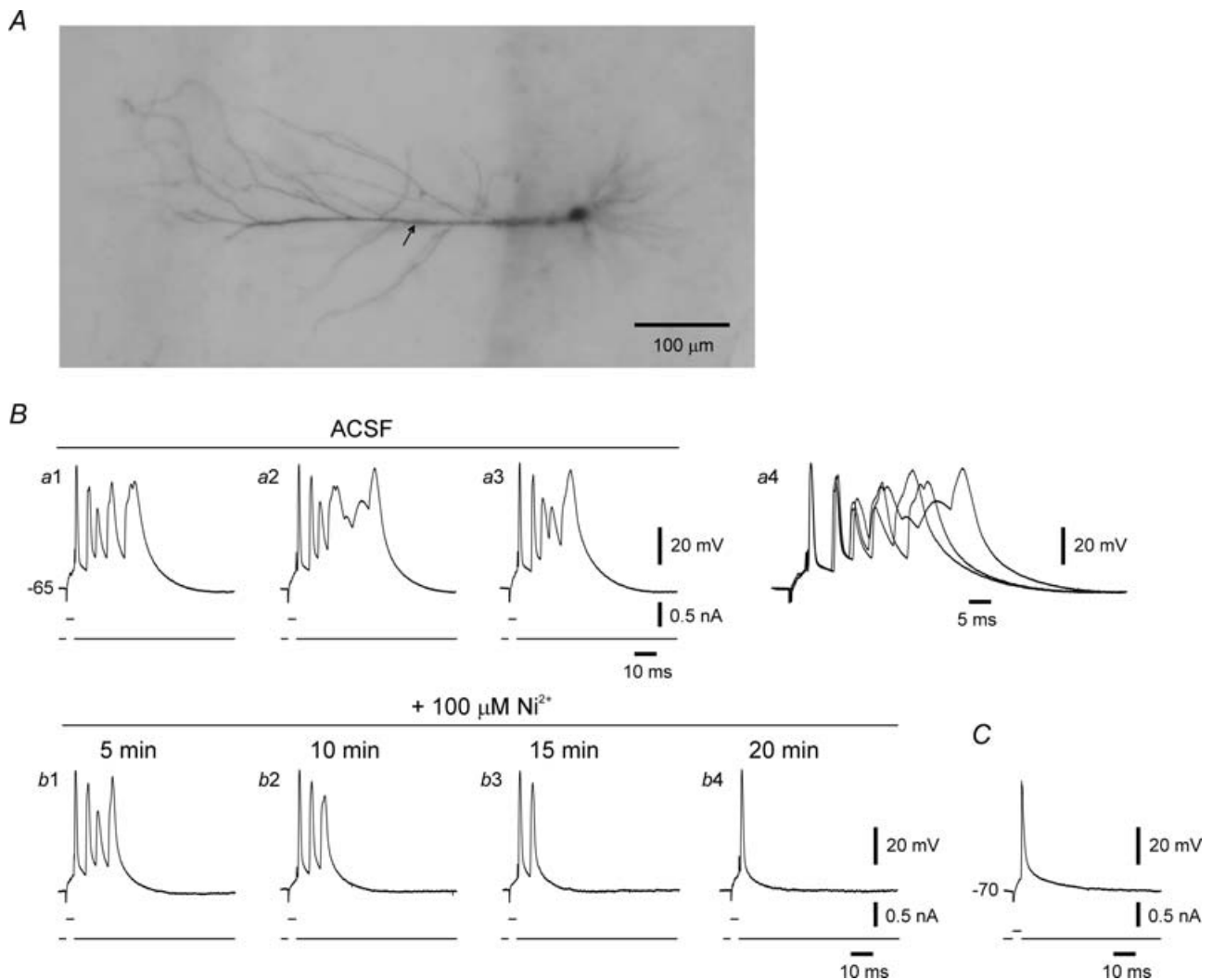

Figure 7. Intradendritic recordings from SE-experienced and control CA1 pyramidal cell
A, photomicrograph shows a biocytin-stained SE-experienced neuron, clearly a pyramidal cell, that was impaled in stratum radiatum at about 200 μm from the pyramidal layer. The approximate site of recording is indicated with arrow. *B*, recordings from the neuron shown in *A*. Brief stimuli evoked bursts of three fast spikes followed by several irregular slow spikes (*a1–a3*; these traces are expanded and overlaid in *a4* to facilitate comparison). Note marked jitter in timing of slow spikes. Adding 100 μM Ni^{2+} to the ACSF first suppressed the slow spikes and eventually reduced the burst to a single spike (*b1–b4*). *C*, intradendritic recordings from a control neuron, identified by biocytin staining as a pyramidal cell. The neuron fired single spikes in response to brief stimuli.

between epilepstogenesis and ontogenesis, suggesting that the emergence of bursting in SE-experienced neurons may be a pathological replay of a normal developmental programme.

Critical role of I_{CaT} in bursting

We have shown previously that bursting in SE-experienced CA1 pyramidal cells (examined 2–6 weeks after pilocarpine-SE) is suppressed in most cases by inhibiting voltage-gated Ca^{2+} currents (Sanabria *et al.* 2001). Further experiments with type-selective Ca^{2+} channel blockers indicated that bursting is unaffected by blockers of L-, N-, P- and Q-type Ca^{2+} currents, but is readily suppressed by 50 or 100 μM Ni^{2+} (Su *et al.* 2002). At these low concentrations, Ni^{2+} blocks I_{CaT} (particularly the $Ca_V3.2$ isoform), as well as I_{CaR} (Williams *et al.* 1999; Lee *et al.* 1999). The latter finding is replicated here also in neurons examined 1 week after pilocarpine-SE (Fig. 1).

Several experimental findings point to the predominant role of I_{CaT} in the bursting of SE-experienced CA1 pyramidal cells. Firstly, the density of I_{CaT} is markedly

($\sim$3-fold) up-regulated after pilocarpine-SE, while that of I_{CaR} is unchanged (Su *et al.* 2002). Secondly, modest depolarization, which causes steady-state inactivation of I_{CaT} but not of I_{CaR} (Randall & Tsien, 1997), abolishes bursting (Su *et al.* 2002). Thirdly, as shown above (Fig. 2), the I_{CaT} blocker amiloride suppresses bursting, whereas the I_R blocker SNX-482 does not. However, because I_{CaR} is only partially blocked by SNX-482 (Sochivko *et al.* 2003), our results do not exclude an auxiliary role for I_{CaR} in bursting.

In normal adult CA1 pyramidal cells, the spike ADP is smaller than in SE-experienced neurons and is insensitive to Ni^{2+} (Su *et al.* 2002; Yue *et al.* 2005), indicating that I_{CaT} is not involved in its generation. Rather, I_{NaP} furnishes the main driving force for the spike ADP (Yue *et al.* 2005). Likewise, I_{NaP} drives bursting induced acutely in these neurons by various experimental manipulations that augment the spike ADP (Azouz *et al.* 1996; Alroy *et al.* 1997; Su *et al.* 2001; Yue & Yaari, 2006). Nevertheless, we show here that despite the critical role of I_{NaP} in shaping the firing mode of normal adult neurons, PDB and riluzole, at concentrations that block I_{NaP} entirely (Yue *et al.* 2005),
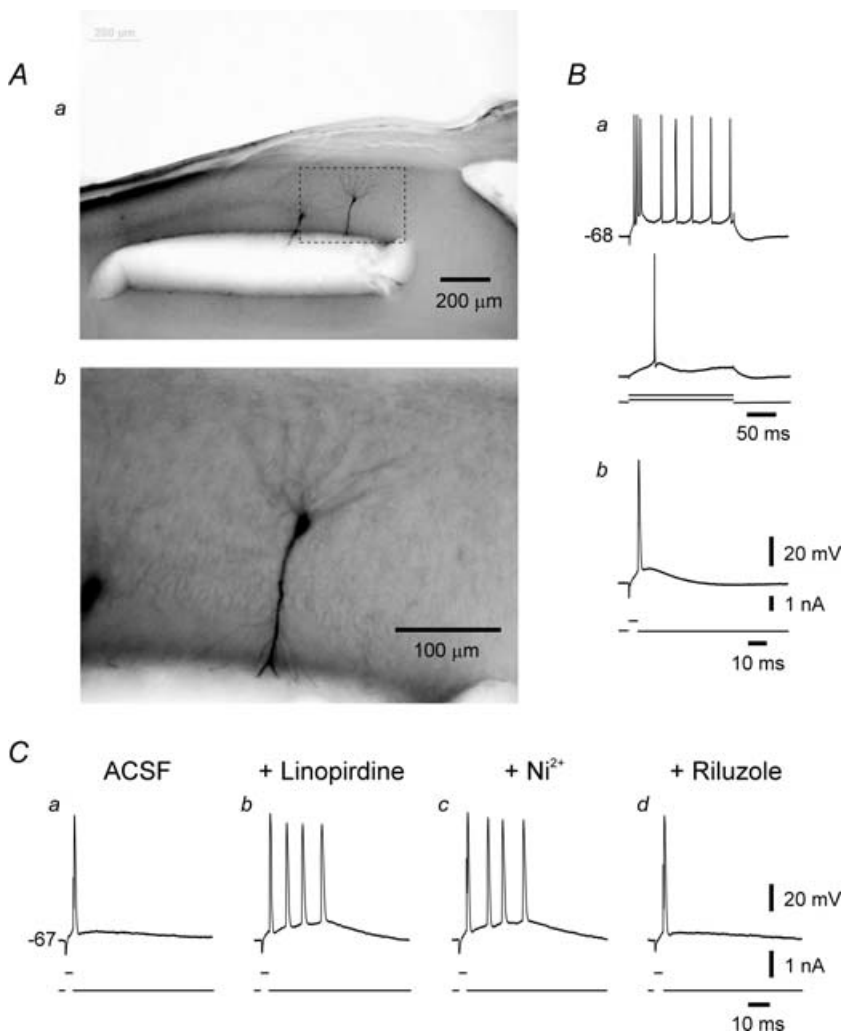

Figure 8. Firing pattern of an SE-experienced CA1 pyramidal cell after truncation of its apical dendrites

A, photomicrograph (*Aa*) shows two neighbouring neurons injected with biocytin through the recording microelectrode about 1 h after severing the apical dendrites by a cut made in stratum radiatum about 150 μm from the pyramidal layer. The biocytin stains the somata, the basal dendrites and the proximal stumps of the apical dendrites of these neurons. The area with in the dashed rectangle in *Aa* is enlarged in *Ab*. *B*, recordings from the truncated neuron shown in *Ab* show high-threshold bursting behaviour (*Ba*). Brief stimuli evoke single spikes in this neuron (*Bb*). *C*, in another similarly truncated SE-experienced neuron, single spikes (*Ca*) are converted to bursts about 20 min after adding 10 μM linopirdine to the ACSF (*Cb*). The linopirdine-induced bursting is resistant to 100 μM Ni^{2+} applied for 30 min (*Cc*), but is readily suppressed by 10 μM riluzole (*Cd*).

do not modify bursting in most SE-experienced neurons (Fig. 3). Thus, I_{NaP} activation generally is not required for bursting. Only in the small subset of bursters (~20%) that do not respond to Ni^{2+}, I_{NaP} probably provides the main driving force for bursting.

'Ping-pong' mechanism of bursting

The fact that I_{CaT} and I_{NaP} can independently drive bursting in the same type of neuron, albeit in different conditions, is likely to be due to their differential spatial distribution. Whereas T-type Ca^{2+} channels are expressed mainly in the distal trunk and oblique processes of apical dendrites (Karst et al. 1993; Christie et al. 1995; Frick et al. 2003), persistent Na^+ channels are expressed largely in the proximal axo-soma (Yue & Yaari, 2006; Golomb et al. 2006), perhaps only in the initial axon segment (Astman et al. 2006). We have shown previously, that I_{NaP}-driven bursting commences in the axo-soma and persists in truncated neurons (Yue et al. 2005; Yue & Yaari, 2006; Golomb et al. 2006). Here we provide ample evidence that the I_{CaT}-driven bursting involves interplay between electrical events in axo-soma and apical dendrites. Firstly, focal application of Ni^{2+} was effective in suppressing bursting when targeted to the distal apical dendrites, but not to the axo-soma (Fig. 4). Secondly, bursting was suppressed by distally applied TTX to block backpropagating spikes (Fig. 5). Thirdly, bursting was suppressed by distally applied retigabine to decrease the excitability of the apical dendrites (Fig. 6; Yue & Yaari, 2006). Fourthly, intra-dendritic recordings revealed Ni^{2+}-sensitive slow spikes associated with bursting (Fig. 7). Finally, severing the distal apical dendrites eliminated bursting (Fig. 8). These data support a 'ping-pong' mechanism of bursting, which commences when the somatic spike backpropagates into the apical dendrites, causing a local depolarization, or even a regenerative slow spike, by recruiting I_{CaT}. The distal I_{CaT}-driven depolarization, in turn, spreads back to the axo-soma, boosting the spike ADP and triggering additional fast spikes, which also backpropagate to the dendrites, reinforcing their depolarization, and so forth. This interplay continues until opposing slow K^+ currents repolarize the neuron (Golomb et al. 2006; Sipila et al. 2006).

A similar 'ping-pong' mechanism of bursting can be invoked in ordinary adult CA1 pyramidal cells by treating them with millimolar levels of 4-aminopyridine (Magee & Carruth, 1999). In this case, the formation of a Ca^{2+} spike in the apical dendrites largely by I_{CaT} is attributed to block of A-type K^+ current (I_A) that normally limits the extent of dendritic spike invasion (Hoffman et al. 1997). Interestingly, it was shown recently that active spike invasion of apical dendrites is more extensive in SE-experienced CA1 pyramidal cells from chronically epileptic rats (6 ± 2 months after pilocarpine-SE), perhaps due to down-regulation of I_A (Bernard et al. 2004). If such a change occurs early in epileptogenesis, it would complement the increase in I_{CaT} density in driving apical dendritic Ca^{2+} spikes and bursting.

Implications for epileptogenesis

The factors that couple pilocarpine-SE to the increase in I_{CaT} density and hence to the emergence of bursting are unknown, but are likely to involve transcriptional and/or post-translational increases in $Ca_V3.2$ expression. It is noteworthy that during the second and third weeks of postnatal development, most CA1 pyramidal cells transiently express a bursting phenotype that also involves recruitment of apical dendritic Ni^{2+}-sensitive Ca^{2+} channels by the backpropagating somatic spikes (Chen et al. 2005). Intriguingly intrinsic bursting behaviour in these developing neurons emerges after a period of intense population bursting (Garaschuk et al. 1998). It would be interesting to determine whether this natural seizure-like activity has a causative role in the subsequent emergence of low-threshold bursting. If that is the case, then the induction of bursting behaviour by pilocarpine-SE may be a pathological replay of a normal development process (Cohen et al. 2003).

A large body of evidence suggests that intrinsic bursters are pivotal to the generation of interictal-like population bursts that occur in between and during epileptic seizures (Yaari & Beck, 2002). In particular, spontaneously bursting neurons are critically important in entraining other neurons into synchronized population bursts, and thus may serve as the initiators and pacemakers of epileptic discharges (Traub et al. 1987; Chagnac-Amitai & Connors, 1989; Jensen & Yaari, 1997). We have shown previously in the pilocarpine-SE model, that bursting neurons drive the entire CA1 network into interictal-like population bursts (Sanabria et al. 2001). It is therefore very likely that the early emergence of intrinsic bursters, perhaps in conjunction with reduced GABAergic inhibition (Dudek et al. 2002), fosters the appearance of interictal EEG 'spikes' early in epileptogenesis (Stewart & Leung, 2003).

Although in this study we have used brief depolarizing current injections to evoke burst discharges, threshold-straddling excitatory postsynaptic potentials (EPSPs) similarly evoke full-blown bursts in bursting neurons (Su et al. 2002). Because postsynaptic bursts induce long-term potentiation of EPSPs (Thomas et al. 1998; Pike et al. 1999), the emergence of bursting early after pilocarpine-SE, may secondarily induce persistent increases in excitatory synaptic transmission that will further lower the threshold for seizure generation (Staley et al. 2005).

In summary, we show that within a few days after pilocarpine-SE, the intrinsic firing mode of 65% of CA1 pyramidal cells shifts from regular firing to bursting. This dramatic change is accounted for mainly by up-regulation of I_{CaT}, whose recruitment in the apical dendrites by backpropagating somatic spikes boosts the somatic spike ADPs to the point of bursting. The appearance of such a large proportion of abnormally firing, or 'epileptic', neurons during the latent period of epileptogenesis, undoubtedly contributes directly and indirectly to the eventual development of a chronic epileptic condition. T-type Ca^{2+} channels (particularly $Ca_V3.2$) are thus identified as potential targets for pharmacological and molecular treatments aimed at halting epileptogenesis during its latent phase.

References

Astman N, Gutnick MJ & Fleidervish IA (2006). Persistent sodium current in layer 5 neocortical neurons is primarily generated in the proximal axon. *J Neurosci* **26**, 3465–3473.

Azouz R, Jensen MS & Yaari Y (1996). Ionic basis of spike after-depolarization and burst generation in adult rat hippocampal CA1 pyramidal cells. *J Physiol* **492**, 211–223.

Bernard C, Anderson A, Becker A, Poolos NP, Beck H & Johnston D (2004). Acquired dendritic channelopathy in temporal lobe epilepsy. *Science* **305**, 532–535.

Chagnac-Amitai Y & Connors BW (1989). Synchronized excitation and inhibition driven by intrinsically bursting neurons in neocortex. *J Neurophysiol* **62**, 1149–1162.

Chen S, Yue C & Yaari Y (2005). A transitional period of Ca^{2+}-dependent bursting triggered by spike backpropagation into apical dendrites in developing rat CA1 neurons. *J Physiol* **567**, 79–93.

Christie BR, Eliot LS, Ito K, Miyakawa H & Johnston D (1995). Different Ca^{2+} channels in soma and dendrites of hippocampal neurons mediate spike-induced Ca^{2+} influx. *J Neurophysiol* **73**, 2553–2557.

Cohen I, Navarro V, Le Duigou C & Miles R (2003). Mesial temporal lobe epilepsy: a pathological replay of developmental mechanisms? *Biol Cell* **95**, 329–333.

Dudek FE, Hellier JL, Williams PA, Ferraro DJ & Staley KJ (2002). The course of cellular alterations associated with the development of spontaneous seizures after status epilepticus. *Prog Brain Res* **135**, 53–65.

Engel J Jr, Williamson PD & Wieser H-G (1997). Mesial temporal epilepsy. In *Epilepsy: a Comprehensive Textbook*, ed.Engel J Jr & Pedley TA, pp. 2417–2426. Lippincott-Taven Publishers, Philadelphia.

French CR, Sah P, Buckett KJ & Gage PW (1990). A voltage-dependent persistent sodium current in mammalian hippocampal neurons. *J Gen Physiol* **95**, 1139–1157.

Frick A, Magee J, Koester HJ, Migliore M & Johnston D (2003). Normalization of Ca^{2+} signals by small oblique dendrites of CA1 pyramidal neurons. *J Neurosci* **23**, 3243–3250.

Garaschuk O, Hanse E & Konnerth A (1998). Developmental profile and synaptic origin of early network oscillations in the CA1 region of rat neonatal hippocampus. *J Physiol* **507**, 219–236.

Golomb D, Yue C & Yaari Y (2006). Contribution of persistent Na^+ current and M-type K^+ current to somatic bursting in CA1 pyramidal cells: combined experimental and modeling study. *J Neurophysiol* **96**, 1912–1926.

Hammarstrom AK & Gage PW (1998). Inhibition of oxidative metabolism increases persistent sodium current in rat CA1 hippocampal neurons. *J Physiol* **510**, 735–741.

Hilaire C, Diochot S, Desmadryl G, Richard S & Valmier J (1997). Toxin-resistant calcium currents in embryonic mouse sensory neurons. *Neurosci* **80**, 267–276.

Hoffman DA, Magee JC, Colbert CM & Johnston D (1997). K^+ channel regulation of signal propagation in dendrites of hippocampal pyramidal neurons. *Nature* **387**, 869–875.

Ikeda M & Matsumoto S (2003). Classification of voltage-dependent Ca^{2+} channels in trigeminal ganglion neurons from neonatal rats. *Life Sci* **73**, 1175–1187.

Jensen MS, Azouz R & Yaari Y (1994). Variant firing patterns in rat hippocampal pyramidal cells modulated by extracellular potassium. *J Neurophysiol* **71**, 831–839.

Jensen MS, Azouz R & Yaari Y (1996). Spike after-depolarization and burst generation in adult rat hippocampal CA1 pyramidal cells. *J Physiol* **492**, 199–210.

Jensen MS & Yaari Y (1997). Role of intrinsic burst firing, potassium accumulation, and electrical coupling in the elevated potassium model of hippocampal epilepsy. *J Neurophysiol* **77**, 1224–1233.

Karst H, Joels M & Wadman WJ (1993). Low-threshold calcium current in dendrites of the adult rat hippocampus. *Neurosci Lett* **164**, 154–158.

Kim HC & Chung MK (1999). Voltage-dependent sodium and calcium currents in acutely isolated adult rat trigeminal root ganglion neurons. *J Neurophysiol* **81**, 1123–1134.

Kleyman TR & Cragoe EJ Jr (1988). Amiloride and its analogs as tools in the study of ion transport. *J Membr Biol* **105**, 1–21.

Lacinová L, Klugbauer N & Hofmann F (2000). Regulation of the calcium channel α_{1G} subunit by divalent cations and organic blockers. *Neuropharmacology* **39**, 1254–1266.

Lee JH, Gomora JC, Cribbs LL & Perez-Reyes E (1999). Nickel block of three cloned T-type calcium channels: low concentrations selectively block α_{1H}. *Biophys J* **77**, 3034–3042.

Magee JC & Carruth M (1999). Dendritic voltage-gated ion channels regulate the action potential firing mode of hippocampal CA1 pyramidal neurons. *J Neurophysiol* **82**, 1895–1901.

Main MJ, Cryan JE, Dupere JR, Cox B, Clare JJ & Burbidge SA (2000). Modulation of KCNQ2/3 potassium channels by the novel anticonvulsant retigabine. *Mol Pharmacol* **58**, 253–262.

Morimoto K, Fahnestock M & Racine RJ (2004). Kindling and status epilepticus models of epilepsy: rewiring the brain. *Prog Neurobiol* **73**, 1–60.

Newcomb R, Szoke B, Palma A, Wang G, Chen X, Hopkins W *et al.* (1998). Selective peptide antagonist of the class E calcium channel from the venom of the tarantula *Hysterocrates gigas*. *Biochemistry* **37**, 15353–15362.

Pike FG, Meredith RM, Olding AW & Paulsen O (1999). Postsynaptic bursting is essential for 'Hebbian' induction of associative long-term potentiation at excitatory synapses in rat hippocampus. *J Physiol* **518**, 571–576.

Priel MR, dos Santos NF & Cavalheiro EA (1996). Developmental aspects of the pilocarpine model of epilepsy. *Epilepsy Res* **26**, 115–121.

Randall AD & Tsien RW (1997). Contrasting biophysical and pharmacological properties of T-type and R-type calcium channels. *Neuropharmacology* **36**, 879–893.

Robbins J (2001). KCNQ potassium channels: physiology, pathophysiology, and pharmacology. *Pharmacol Ther* **90**, 1–19.

Sanabria ER, da Silva AV, Spreafico R & Cavalheiro EA (2002). Damage, reorganization, and abnormal neocortical hyperexcitability in the pilocarpine model of temporal lobe epilepsy. *Epilepsia* **43** (Suppl. 5), 96–106.

Sanabria ER, Su H & Yaari Y (2001). Initiation of network bursts by Ca^{2+}-dependent intrinsic bursting in the rat pilocarpine model of temporal lobe epilepsy. *J Physiol* **532**, 205–216.

Scroggs RS & Fox AP (1992). Calcium current variation between acutely isolated adult rat dorsal root ganglion neurons of different size. *J Physiol* **445**, 639–658.

Sipila ST, Huttu K, Voipio J & Kaila K (2006). Intrinsic bursting of immature CA3 pyramidal neurons and consequent giant depolarizing potentials are driven by a persistent Na^+ current and terminated by a slow Ca^{2+}-activated K^+ current. *Eur J Neurosci* **23**, 2330–2338.

Sochivko D, Chen J, Becker A & Beck H (2003). Blocker-resistant Ca^{2+} currents in rat CA1 hippocampal pyramidal neurons. *Neuroscience* **116**, 629–638.

Sochivko D, Pereverzev A, Smyth N, Gissel C, Schneider T & Beck H (2002). The $Ca_V2.3$ Ca^{2+} channel subunit contributes to R-type Ca^{2+} currents in murine hippocampal and neocortical neurones. *J Physiol* **542**, 699–710.

Spruston N, Schiller Y, Stuart G & Sakmann B (1995). Activity-dependent action potential invasion and calcium influx into hippocampal CA1 dendrites. *Science* **268**, 297–300.

Staley K, Hellier JL & Dudek FE (2005). Do interictal spikes drive epileptogenesis? *Neuroscientist* **11**, 272–276.

Stewart LS & Leung LS (2003). Temporal lobe seizures alter the amplitude and timing of rat behavioral rhythms. *Epilepsy Behav* **4**, 153–160.

Su H, Alroy G, Kirson ED & Yaari Y (2001). Extracellular calcium modulates persistent sodium current-dependent intrinsic bursting in rat hippocampal neurons. *J Neurosci* **21**, 4173–4182.

Su H, Sochivko D, Becker A, Chen J, Jiang Y, Yaari Y & Beck H (2002). Upregulation of a T-type Ca^{2+} channel causes a long-lasting modification of neuronal firing mode after status epilepticus. *J Neurosci* **22**, 3645–3655.

Takahashi K, Wakamori M & Akaike N (1989). Hippocampal CA1 pyramidal cells of rats have four voltage-dependent calcium conductances. *Neurosci Lett* **104**, 229–234.

Tang CM, Presser F & Morad M (1988). Amiloride selectively blocks the low threshold (T) calcium channel. *Science* **240**, 213–215.

Tatulian L, Delmas P, Abogadie FC & Brown DA (2001). Activation of expressed KCNQ potassium currents and native neuronal M-type potassium currents by the anticonvulsant drug retigabine. *J Neurosci* **21**, 5535–5545.

Thomas MJ, Watabe AM, Moody TD, Makhinson M & O'Dell TJ (1998). Postsynaptic complex spike bursting enables the induction of LTP by theta frequency synaptic stimulation. *J Neurosci* **18**, 7118–7126.

Todorovic SM & Lingle CJ (1998). Pharmacological properties of T-type Ca^{2+} current in adult rat sensory neurons: effects of anticonvulsant and anesthetic agents. *J Neurophysiol* **79**, 240–252.

Tottene A, Volsen S & Pietrobon D (2000). α_{1E} subunits form the pore of three cerebellar R-type calcium channels with different pharmacological and permeation properties. *J Neurosci* **20**, 171–178.

Traub RD, Miles R & Wong RK (1987). Models of synchronized hippocampal bursts in the presence of inhibition. I. Single population events. *J Neurophysiol* **58**, 739–751.

Turski WA, Cavalheiro EA, Schwarz M, Czuczwar SJ, Kleinrok Z & Turski L (1983). Limbic seizures produced by pilocarpine in rats: behavioural, electroencephalographic and neuropathological study. *Behav Brain Res* **9**, 315–335.

Waldmann R, Champigny G, Bassilana F, Heurteaux C & Lazdunski M (1997). A proton-gated cation channel involved in acid-sensing. *Nature* **386**, 173–177.

Wellmer J, Su H, Beck H & Yaari Y (2002). Long-lasting modification of intrinsic discharge properties in subicular neurons following status epilepticus. *Eur J Neurosci* **16**, 259–266.

Wickenden AD, Yu W, Zou A, Jegla T & Wagoner PK (2000). Retigabine, a novel anti-convulsant, enhances activation of KCNQ2/Q3 potassium channels. *Mol Pharmacol* **58**, 591–600.

Williams ME, Washburn MS, Hans M, Urrutia A, Brust PF, Prodanovich P, Harpold MM & Stauderman KA (1999). Structure and functional characterization of a novel human low-voltage activated calcium channel. *J Neurochem* **72**, 791–799.

Williams S, Serafin M, Muhlethaler M & Bernheim L (1997). Distinct contributions of high- and low-voltage-activated calcium currents to afterhyperpolarizations in cholinergic nucleus basalis neurons of the guinea pig. *J Neurosci* **17**, 7307–7315.

Wilson SM, Toth PT, Oh SB, Gillard SE, Volsen S, Ren D, Philipson LH, Lee EC, Fletcher CF, Tessarollo L, Copeland NG, Jenkins NA & Miller RJ (2000). The status of voltage-dependent calcium channels in α_{1E} knock-out mice. *J Neurosci* **20**, 8566–8571.

Yaari Y & Beck H (2002). 'Epileptic neurons' in temporal lobe epilepsy. *Brain Pathol* **12**, 234–239.

Yue C, Remy S, Su H, Beck H & Yaari Y (2005). Proximal persistent Na^+ channels drive spike afterdepolarizations and associated bursting in adult CA1 pyramidal cells. *J Neurosci* **25**, 9704–9720.

Yue C & Yaari Y (2004). KCNQ/M channels control spike afterdepolarization and burst generation in hippocampal neurons. *J Neurosci* **24**, 4614–4624.

Yue C & Yaari Y (2006). Axo-somatic and apical dendritic Kv7/M channels differentially regulate the intrinsic excitability of adult rat CA1 pyramidal cells. *J Neurophysiol* **95**, 3480–3495.